Supplementary Information

1 Microroller speed against rotational frequencies

We measure the microroller speed as a function of the applied rotational frequency. We carry the pattern experiments in the frequency range to which the speed is proportional to make sure that the applied torque is the dominant mechanism of the microroller translation.
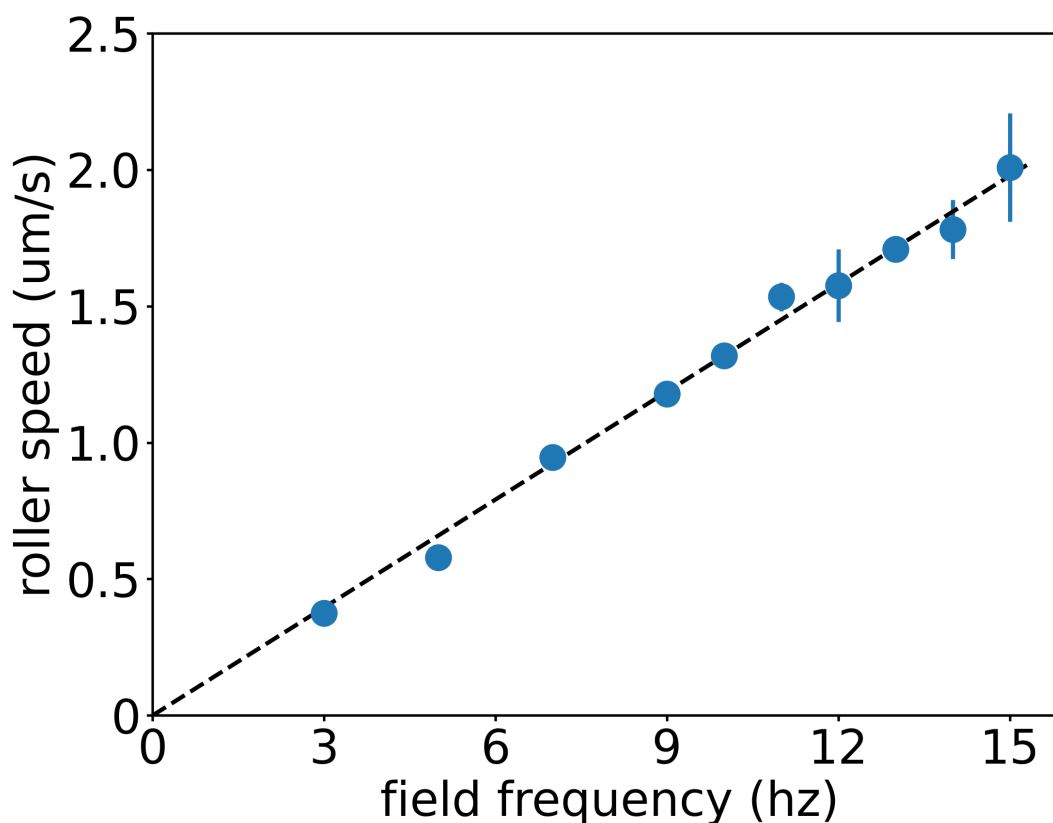

Figure S1: **Microroller speed is proportional to the applied frequency.** We make a microroller water suspension with low concentration (few microrollers within the field of view), and apply a rotational magnetic field with a constant field strength (80 Gs) in a range of frequencies. Then, we measure the average speed of the microrollers and fit a straight line across the whole data set. The black dashed line shows the fitting result; the slope of the line is 0.13 μm.

2 Microroller displacement in a passive suspension

Fig. S2 shows the microroller displacement in a passive colloidal suspension with two rotational frequencies.
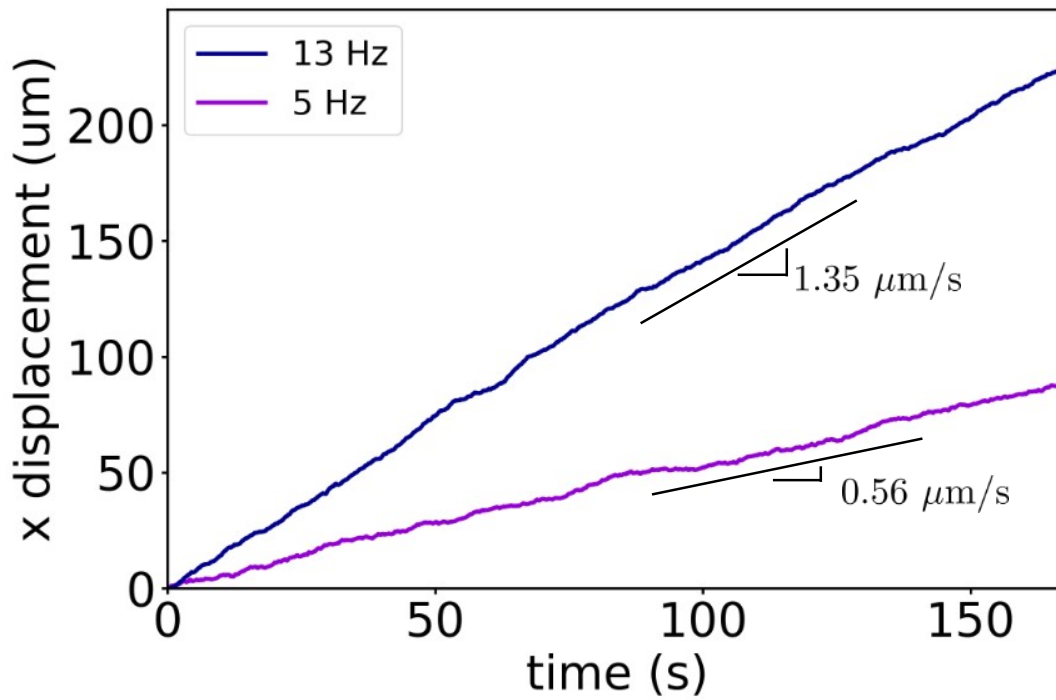

Figure S2: **Microroller speed is constant in the colloidal suspension.** We track the displacement of a microroller in a suspension ($\phi_{area} = 0.16\%$) that is driven by two different frequencies. We find that the speed is constant and is again proportional to the rotational frequency.

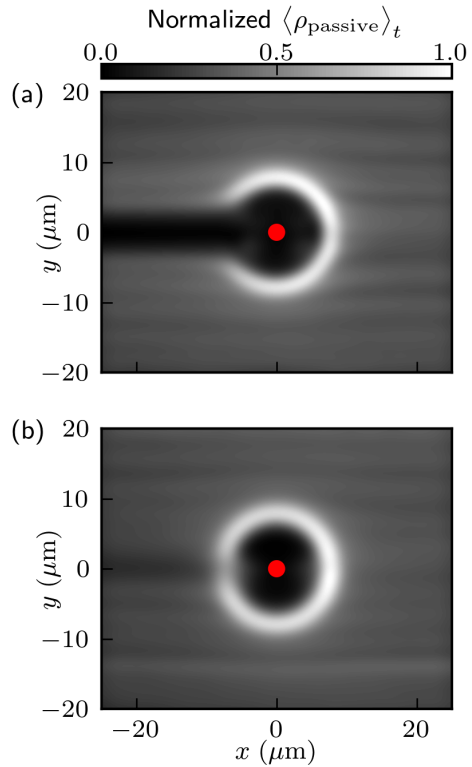# 3   Depletion region is affected by the mass of the passive particles

Figure S3: **The depletion region is strongly affected by gravitational forces on the passive particles.** We performed two sets of simulations where we independently turn of near-field interactions and gravitational forces. In (a) we show the emergent pattern from simulations without near-field interactions between particles. The depletion region is unaffected by near-field interactions as it is still present in the pattern. Meanwhile, (b) is the emergent pattern from simulations with mass-less passive particles and observe that the depletion region is largely affected.

4 Supporting Tables

Parameter	Value	Units
Microroller radius	1.0×10^{-6}	m
Passive particle radius	1.0×10^{-6}	m
Microroller buoyant mass	3.1×10^{-15}	kg
Passive particle buoyant mass	2.5×10^{-16}	kg
Water viscosity	0.001	Pa s
ϵ_{cut}	2×10^{-21}	J
κ_{cut}	0.001×10^{-6}	m
Particle-particle $r_{\text{cutoff}}^{\text{Lubtication}}$	5×10^{-6}	m
Particle-particle $r_{\text{cutoff}}^{\text{Lubrication}}$	10^4	m
GMRES solver tolerance	10^{-6}	(dimensionless)
$\tau_{y\,\text{max}}$	4.0×10^{-18}	N m

Table 1: Parameters used in all simulations.

$\epsilon\,(10^{-18}\,J)$	$\kappa\,(\mu\text{m})$	height (μm)
0.0386	0.0756	1.212
0.0526	0.0816	1.246
0.029	0.29	1.339
0.06	0.17	1.415
0.06	0.21	1.467
0.08	0.19	1.498
0.12	0.21	1.615
0.19	0.22	1.734
0.29	0.23	1.853

Table 2: Yukawa type potential parameters used in simulations to produce different microroller heights at $T = 0\,\text{K}$.

$\epsilon\,(10^{-18}\,J)$	$\kappa\,(\mu\mathrm{m})$	height $(\mu\mathrm{m})$
0.00386	0.0756	1.229
0.00526	0.0816	1.266
0.0029	0.29	1.406
0.006	0.17	1.453
0.006	0.21	1.515
0.008	0.19	1.539
0.012	0.21	1.661
0.019	0.22	1.782
0.029	0.23	1.905

Table 3: Yukawa type potential parameters used in simulations to produce different passive particle heights at $\mathrm{T} = 0\,\mathrm{K}$.

$\epsilon\,(10^{-18}\,J)$	$\kappa\,(\mu\mathrm{m})$	Average height $(\mu\mathrm{m})$
0.0386	0.0756	1.305 ± 0.143
0.0526	0.0816	1.335 ± 0.147
0.0346	0.1036	1.339 ± 0.158
0.029	0.29	1.394 ± 0.215

Table 4: Yukawa type potential parameters used in simulations to produce different microroller heights at $\mathrm{T} = 293\,\mathrm{K}$.

$\epsilon\,(10^{-18}\,J)$	$\kappa\,(\mu\mathrm{m})$	Average height $(\mu\mathrm{m})$
0.00386	0.0756	1.964 ± 0.915
0.00526	0.0816	2.020 ± 0.939
0.00346	0.1036	1.973 ± 0.924
0.0029	0.29	2.1189103 ± 1.006

Table 5: Yukawa type potential parameters used in simulations to produce different passive particle heights at $\mathrm{T} = 293\,\mathrm{K}$.